Evaluation of the DIAL technique for studies on NO_2 using a mobile lidar system

Kent A. Fredriksson and Hans M. Hertz

The DIAL technique for remote monitoring of nitrogen dioxide is evaluated. A comprehensive field test and evaluation program was performed to determine the measuring capability for this pollutant. The potential sources of error are discussed and these are analyzed for the mobile lidar system used in the work. This system employs a dye laser pumped by a Nd:YAG laser; a laser source which has improved the measuring accuracy compared with earlier work on nitrogen dioxide. The accuracies are found to be good enough for measuring needs in many studies on air pollution problems. A few typical examples of measurements from the field test program are given.

I. Introduction

The DIAL technique has proved to be useful for remote monitoring of atmospheric pollutants. Research teams have demonstrated measurements on several molecules, e.g., SO_2, O_3, NO_2, Hg, NO, C_2H_4, CO, H_2O, and CH_4.[1] The lidar research within our group was initiated in 1975 and several early field tests were carried out.[2] In 1979 a mobile lidar system was constructed which was presented in a detailed paper.[3] The system was evaluated and tested for two and a half years and a summary report containing a number of conclusions was written.[4] A paper focused on strategies and routines for DIAL measurements on SO_2 has also been presented.[5] In this work the DIAL technique was analyzed with special regard to measurements on NO_2. Several field tests and experiments to determine the measurement accuracies were made and examples from these are presented in this paper. Potential systematic errors and signal-to-noise ratios in DIAL measurements are discussed, and comparisons are made with the mobile system in practical applications.

The first DIAL experiments on NO_2 were made in 1973–74 by Rothe *et al.*[6] and by Grant *et al.*[7] In 1979 Baumgartner *et al.*[8] conducted a study on NO_2 in which the DIAL measurements were compared to a conventional point monitoring system. These early studies were all made with flashlamp-pumped dye lasers and, with respect to the high consumption of coumarin dyes in such lasers, it is not likely that such lasers can be used for routine measurements on NO_2. In addition evaluations of the NO_2 measurement accuracy were presented, which were quite discouraging in view of the measurement needs (e.g., Ref. 9). NO_2 DIAL measurements were made by our group in 1976 employing a dye laser pumped by a nitrogen laser. The limitation in this case was the low laser pulse power, which made daytime measurements difficult. With the availability of Nd:YAG laser-pumped dye lasers, which we obtained in 1979, the practical aspects of the NO_2 DIAL technique were improved. It is now possible to do daytime measurements of source emissions, background concentrations, and concentrations in metropolitan areas, and the detection limits and accuracies of the remote sensing is comparable with those of conventional point monitoring instruments.

II. NO_2 Pollutant

During the last few decades nitrogen oxides have emerged as one of our major air pollution problems. The emissions of nitrogen oxides were estimated to have doubled in the major Swedish cities from 1960 to 1980. Except for their direct toxicity, they cause acidification of water, play an important role in the formation of photochemical smog, and are active in atmospheric chemical reactions.

The nitrogen oxides are emitted primarily from three types of source: the burning of fossil fuels, industrial processes at nitric acid plants, e.g., artificial fertilizer plants and explosives plants, and motor vehicle traffic. The bulk of the nitrogen oxides (NO_x) is emitted as the nontoxic compound NO, which is formed in high temperature reactions between nitrogen and oxygen. When NO is emitted into the atmosphere, it is oxidized

The authors are with Lund Institute of Technology, Physics Department, Center for Laser Studies of the Environment, P.O. Box 725, S-220 07 Lund, Sweden.

Received 18 October 1983.
0003-6935/84/091403-09$02.00/0.

with O_2 and O_3 to NO_2. The reaction with O_3 is nearly instantaneous, whereas oxidization with O_2 is slow and depends strongly on the NO concentration. The half-life of 1-ppm NO is ~100 h and of 0.1 ppm ten times longer.[10] In the atmosphere the NO and NO_2 are engaged in a complicated set of reactions forming compounds such as HNO_2, HNO_3, and NO_3. The complex NO_x chemistry is currently under investigation by many groups.

It has been shown that NO_2 causes plant injuries at concentrations below 500 $\mu g/m^3$ and may cause difficulties in breathing at 200 $\mu g/m^3$. Some investigations connect the increased occurrence of cancer in metropolitan areas with NO_2. In rain, the gas is dissolved in water forming nitric acid, which has been found to substantially contribute to the acidification problem.

III. Differential Absorption Lidar Technique for Measurements on NO_2

The principle of the differential absorption lidar (DIAL) technique has been described before (e.g., Ref. 11). In this paper the theory is briefly outlined and the details which are important for the accuracy in the practical work are discussed more thoroughly.

In a DIAL measurement the lidar return, backscattered from the atmosphere or a target and collected via a telescope, is studied at two or more wavelengths. The power P of the lidar signal for a wavelength λ from a range interval ΔR at the distance R can be expressed in a simplified form as

$$P_\lambda(R,\Delta R) = C(R) W \sigma_b N(R) \frac{\Delta R}{R^2} \times \exp\left\{-2 \int_0^R [\sigma(\lambda) n(r) + \sigma_a N(r)] dr\right\}. \quad (1)$$

In this equation $C(R)$ is a system function, W is the transmitted laser pulse power, σ_b is the average backscattering cross section of the $N(R)$ scattering objects per unit volume, and the exponential is due to the attenuation by molecules, $n(r)$, and particles, $N(r)$, with absorption cross sections $\sigma(\lambda)$ and σ_a, respectively. When NO_2 is studied, the lidar signal at a wavelength of the absorption spectrum in the blue region, typically 448.1 nm, is measured. A reference measurement is made at a close-lying wavelength, e.g., 446.8 nm, where the absorption cross section for the gas is much lower. Since there are no atmospheric gases with interfering absorption spectra in this spectral region, it is in practical cases sufficient to measure at two wavelengths. The evaluation of the DIAL measurement is made by dividing the two lidar signals for each distance R:

$$\frac{P_{\lambda_{abs}}(R)}{P_{\lambda_{ref}}(R)} = C' \exp\left\{-2 \int_0^R [\sigma(448.1) - \sigma(446.8)] n'(r) dr\right\}, \quad (2)$$

where C' is a new system constant, $\sigma(448.1)$ and $\sigma(446.8)$ are the absorption cross sections at the wavelengths studied, and $n'(r)$ is the NO_2 concentration at the distance r, which is the integration parameter in the integral. The quotient will decrease at the distances where the gas is present and the slope is determined by the concentration.

From the DIAL equation, Eq. (2), the mean concentration of NO_2 is calculated for range intervals R_2–R_1 according to the equation

$$n'(r) = \{2(R_2 - R_1)[\sigma(448.1) - \sigma(446.8)]\}^{-1} \times \ln \frac{P_{\lambda_{abs}}(R_1) P_{\lambda_{ref}}(R_2)}{P_{\lambda_{ref}}(R_1) P_{\lambda_{abs}}(R_2)}. \quad (3)$$

The range interval is swept with the distance R to obtain the concentration profile along the measurement direction. The selected length of the range interval in the calculation, which is the distance resolution in the measurement, depends on the physical situation in the study. When a distinct plume is measured, 10 m can be appropriate, but when an ambient air concentration is studied an interval of several hundred meters is chosen. The detection limit in a DIAL recording can be expressed as the measurable concentration multiplied by the range interval in $mg/m^3 \cdot m$ or $ppm \cdot m$.

The accuracy in a DIAL measurement depends directly, according to Eqs. (2) and (3), on the accuracy in the determination of the differential absorption cross section of the gas at the two wavelengths. In the case of NO_2 this factor, which also demands an accurate knowledge of the measurement wavelengths, can be reduced to a minor source of error. When gases such as NO and Hg with narrow absorption lines in the UV region or gases with spectra in the IR region are measured, the determination of the cross section can be of crucial importance for the accuracy.

In the ideal case the DIAL equation has no distance dependence except for the dependence on the NO_2 concentration along the measurement direction, which is expressed by the integral in Eq. (2). In the actual situation this is not always the case and there may be another differential distance dependence in the lidar signal at the two wavelengths. This dependence, which can be described by $C'(R)$ in Eq. (2), might cause a systematic error in the measurements. The sources for such a dependence will be discussed here, and in the following sections our special system and applications of the technique will be discussed in this respect.

A very important detail to consider in a DIAL system is the overlap of the transmitted laser beam with the telescope field of view. The overlap generally has a distance dependence, which is included in the system function $C(R)$ in the lidar equation. In principle a slight misalignment of the laser beam compared to the telescope gives no systematic error in a DIAL measurement but merely reduces the signal-to-noise ratio because of the lost efficiency in the detection. However, if one of the two wavelengths has a different overlap with the telescope field of view compared with the other wavelength, a systematic error is introduced. It can be difficult to align the two laser beams exactly if different laser sources are used for the two wavelengths, but even if the same laser is used, differences in the beam direction may occur. Prisms and other wavelength dispersive elements in the laser beam path in the system are a potential source of differential misalignment. For

close-lying wavelengths these effects are normally very small, and with a field of view somewhat larger than the laser beam divergence the problem is negligible. However, in measurements at short distances it is also essential that the spatial intensity distribution of the laser beam be the same for the two wavelengths, since the telescope field of view is limited at short distances. In a coaxial lidar the backscattering at short distances is partly blocked by the folding mirror in the telescope, and thus the overlap will depend on the spatial intensity distribution of the beam. This effect is more important if the two laser beams are generated by different sources. When frequency shifting crystals are employed, e.g., in DIAL measurements on O_3 or SO_2, the spatial distribution is changed, and then the same differential effect exists even with a single-laser source.

The reduced overlap of the laser beam and the telescope field of view at shorter distances is sometimes referred to as geometrical compression of the lidar signal, and the dependence can be described with an overlap or crossover function.[12–15] By changing the overlap function the dynamic range of the signal can be reduced. However, in a DIAL system the effect must be dealt with carefully to avoid systematic errors.

In some cases a topographic target can be utilized to increase the measurement range in a DIAL study. Then a similar problem may appear if the topographic target is nonuniform and if the laser beam cross section is not exactly the same for the two wavelengths.

In the division of the two lidar expressions leading to Eq. (2) it is assumed that the backscattering function $\sigma_b N(r)$ and the attenuation exponential are exactly the same except for the NO_2 dependence. This presumption is true on the average, since there is, in practice, no strong wavelength dependence in the backscattering and there are no interfering absorbing gases at the studied wavelengths. The scattering and attenuation from particles generally have a smooth wavelength dependence as they are well distributed over different sizes and shapes. However, each single lidar signal is unique and reflects the time-varying atmospheric conditions. Thus, one pair of lidar signals should be measured at the same time or at least within tens of microseconds to fulfill the requirements for Eq. (2), and this in turn usually requires two laser sources. If only one laser is used and the lidar signals are separated in time, some period of signal averaging is needed to give comparable recordings. Practically, this means that the laser is alternately tuned to the two wavelengths and with a 10-Hz laser the signals are then 0.1 sec apart. In this work we have shown that this procedure does not cause any difficulties in most measurements on emissions or the ambient air. Some period of averaging is needed anyway to gather enough statistics and to perform a measurement which is representative for the pollution situation.

However, the averaging itself may be a systematic source of error. Generally the lidar signal in the form of Eq. (1) is averaged, but the NO_2 concentration is proportional to minus the logarithm of the signal. When a stable atmospheric situation is present no error is introduced, but if the concentration varies greatly a lower value than the actual mean concentration will be measured. The remedy for this is to avoid measurements of fluctuating high concentrations. If, for example, the flow of a stack plume with high concentration of the studied gas is to be measured, the measurement should be made at some hundred meters from the source, where the plume has spread somewhat and the concentration is lower. Alternatively the logarithm of the signal can be taken before the averaging. In this work the latter technique was not applied but it will be tested in the continuing study. A similar error can occur if the relative power of the two laser beams changes during the averaging. This is not likely to happen in a single-laser system measuring NO_2, but in a system with two lasers or if optical frequency shifting is employed in, e.g., SO_2 measurements, it has to be considered. The effect is of special importance when studying an inhomogeneous atmosphere, e.g., in an industrial area with several diffuse particle plumes.

The DIAL equation, Eq. (2), is based on the assumption that the lidar signals are made up of single-scattering events in the atmosphere. However, in high-turbidity atmospheres multiple scattering contributes considerably to the collected lidar signals, which can introduce a systematic error. When a gaseous content in a dense plume is measured, Eq. (3) then implies a too-low value for the concentration, since the lidar signal representing the distances behind the plume [R_2 in Eq. (3)] is to some extent made up of multiple scattering in the plume. The remedy is to avoid measurements in the dense plume and measure the spreading plume instead. The same source of error appears in studies on distributed gases in very hazy and foggy atmospheres which makes measurements difficult. The multiple scattering can be partly discriminated by placing a polarizer in the detection system, taking advantage of the fact that the plane polarization of an incident laser beam is retained only in the single scattering from spherical particles.[16,17] To our knowledge there have been no systematic studies of such a detection scheme in DIAL measurements, but we plan to test the technique in our continuing work.

Linearity of the signal detection system is essential. In principle a photomultiplier tube, which is used for the detection of the returning light, does not give a signal strictly proportional to the detected number of photons. The nonlinearity is worse for strong signals and must be compensated for. This can be done after the averaging if the signal does not fluctuate appreciably. For weak lidar signals the detection signal is very nearly linear. In nighttime measurements the background level can be extremely low and then a weak signal can be captured in a linear photon counting manner. The transient recorder of the lidar system must be carefully adjusted for a linear response, and it is also essential that the triggering of the recorder is exact. If the gain of the photomultiplier tube is modulated or gated, which it often is to increase the dynamic range of the detection system, it is also important that the modulation be synchronized with the laser pulse.

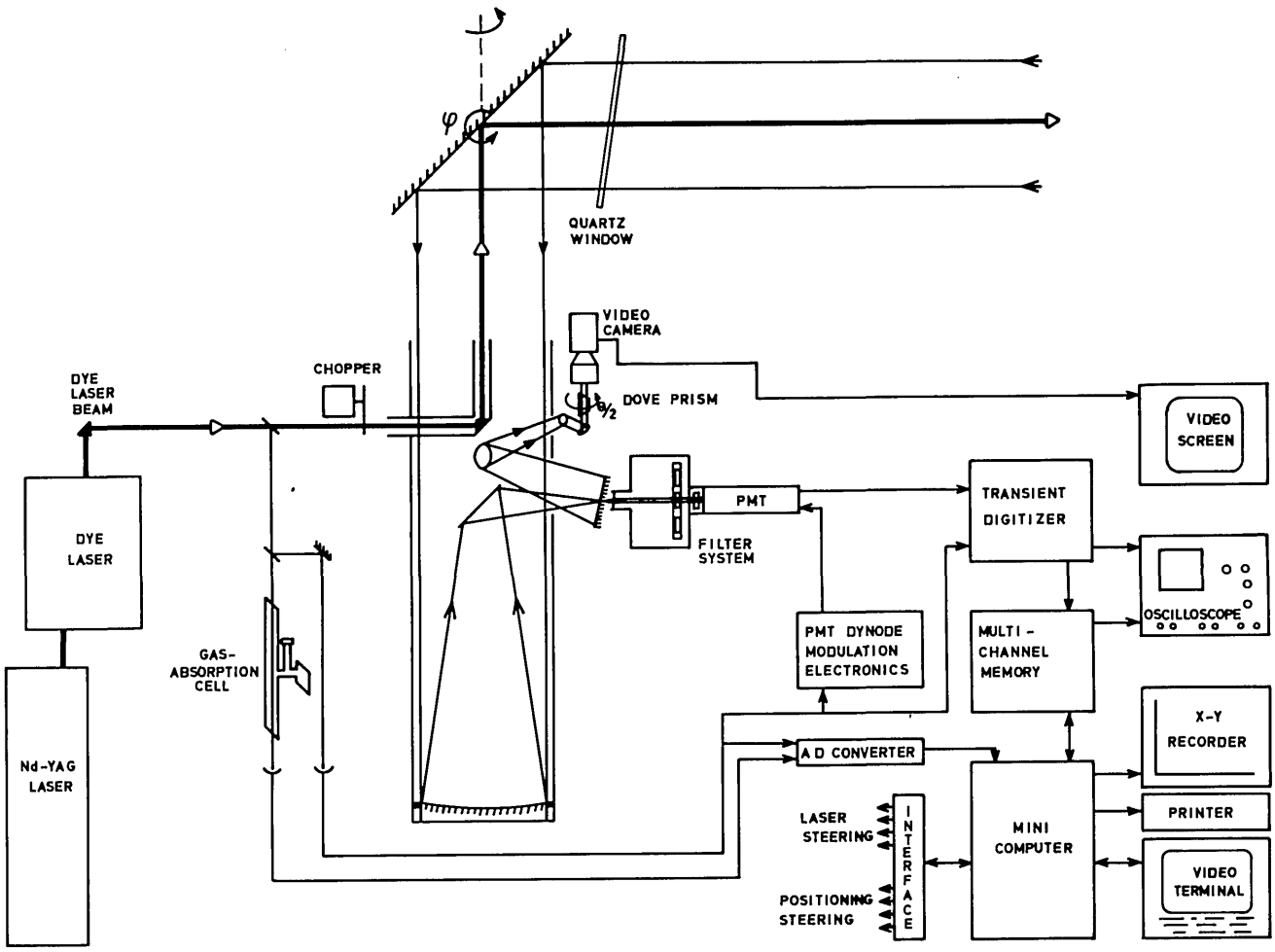

Fig. 1. Schematic diagram of the electronic and optical arrangements of the mobile DIAL system.

IV. Mobile System for NO_2 DIAL Measurements

A mobile lidar system was constructed in 1979 at the Chalmers University in Gothenburg, which at that time was the base for our activities. Figure 1 is a schematic diagram of the system, which has been described in a detailed paper.[3] Some basic parameters for the lidar system are given in Table I. Here we will only discuss the details which are of special interest in applications of the DIAL technique for measurements on NO_2. The accuracies of the technique, which were determined in this work, are typical for those attainable with a dedicated mobile NO_2 DIAL system intended for measurements performed on a routine basis. In some cases the accuracies and especially the measurement ranges may be further improved, but we think that this work is a useful example, which describes the technical and practical capability in routine work on air pollution.

The Nd:YAG laser-pumped dye laser of the mobile system is wavelength calibrated by studying the absorption spectrum of NO_2 in the wavelength region in question. The calibration routine is simple, employing a gas cell which contains a mixture of NO_2 and N_2 at atmospheric pressure, and the procedure is run through before each study. The linearity of the wavelength scale of the laser has also been checked with a monochromator and recently a hollow cathode discharge unit has been included for very precise calibration employing the optogalvanic effect. The spectrum of neon has been utilized for calibration in the 560–600-nm wavelength region, and we are planning to apply a similar technique to other parts of the visible spectrum.

Table I. Basic Parameters of the NO_2 DIAL System

Transmitted pulse energy	1–4 mJ
Pulse duration	~7 nsec
Pulse repetition rate	10 Hz
Laser beam divergence	0.7 mrad
Diameter of the receiving telescope	30 cm
Maximum transmission of the interference filter	54%
Bandwidth of the interference filter	5 nm
Quantum efficiency of the photomultiplier tube	17%
Sample interval of the detection electronics	10 nsec

The rapid wavelength tuning of the dye laser, which changes the wavelength between each shot, is made with a rotating eccentric wheel coupled to the grating of the laser. The laser is fired when the wheel and the tuning angle of the grating are at preset positions. The wheel is turned by a stepping motor with a resolution of 400 steps/revolution.

In the calculations of NO_2 concentrations the absorption cross sections measured by Woods and Jol-

liffe[18] are employed. Since the spectral bandwidth in these measurements was larger than the bandwidth of the laser in our system, we have made some complementary tests.

To confirm the accuracy in the DIAL measurements, the studies of the differential NO_2 spectra were made in a similar way as for an ordinary DIAL recording with exactly the same equipment. A gas cell with 6 g/m^3 of NO_2 in N_2 at atmospheric pressure was put into the laser beam before entering the output optics of the system. The backscattered lidar signal from the atmosphere at a close distance was collected while the computer shifted the wavelength between each laser shot as in a DIAL recording. The wavelength shift was 1.3 nm, which is the usual shift in our NO_2 measurements. The DIAL signal was calculated for different pairs of wavelengths in the region of interest. The measurement points were changed by the basic setting of the dye laser grating, whereas the preset positions of the rapid wavelength shifting unit were the same throughout the test. The interval between the points was chosen to be 8 or 16 pm, which is of the same order of magnitude as the bandwidth of the laser. Additional tests were made to study the small interference effects of the laser intensity which were introduced by the gas cell windows. In this simulation of a DIAL measurement all uncertainties in the differential absorption cross-sectional value were exploited. The differential spectral dependence was compared with the spectrum of Woods and Jolliffe. The conclusion from the study is that the parameter of the differential absorption in our NO_2 measurements is 8.3 (0.5) cm^{-1} atm^{-1}. The error limit also includes the uncertainties in the wavelength calibration and the rapid wavelength shifting system, which together were <0.1 nm. It is possible to further increase the accuracy by determining the exact wavelengths in the measurement, which will be done by optogalvanic calibration.

Since the two laser beams are generated by the same laser and transmitted through the same optical components before leaving the system, they are collinear and there should be no distance dependence in the system parameter C' in Eq. (2). However, there are wavelength dispersive elements in the dye laser and there are two right-angle prisms in the beam path, where the beam might deviate from an exact perpendicular incidence, giving rise to a small wavelength dependence in the beam direction. These effects have been calculated and studied in the practical work and they are found to be negligible at distances larger than 200 m. To make doubly sure, the aperture in the telescope is kept wide enough so that the telescope field of view is somewhat larger than the laser beam divergence. This can be easily checked and adjusted during the measurements. At distances shorter than 200 m we have observed a wavelength dependence of the lidar signal which varies with the precise adjustment of the laser beam direction. A slight misalignment of the two beams or a small difference in the intensity distribution may give a distance dependence since the overlap function of the beam and the telescope field of view may then change drastically. In NO_2 measurements it is possible to carefully adjust the beam direction and avoid this problem with our system. However, in a typical routine measurement such a precise adjustment is not done. In an SO_2 or O_3 DIAL measurement involving different optical components for the two beams, the problem is more difficult to solve.

The photomultiplier tubes in the system are the EMI 9817 type and the units were selected to give a more linear response than average tubes. The one used in this work is equipped with a dynode chain which can be modulated to increase the dynamic range of the measurements. The linearity of the detection system was found to be very good when tested with optical neutral density filters. Furthermore, the fact that the laser power on the two wavelengths is always kept equal ensures that there is no source of systematic error due to any nonlinearity. These tests also involved the transient recorder of the system, a Biomation 8100 unit, which needed an accurate adjustment in order to make it linear when it was included in the system. Since this unit has a dynamic range of 256 steps (8 bits) only, the modulated gain of the photomultiplier tube is essential. In the single-photon detection domain for weak lidar signals it is important that each detected photon gives rise to a few steps. The transient digitizer might otherwise introduce systematic errors in the form of irregularities in the averaged lidar curve.

The transient recorder is triggered by a pulse generator which also triggers the Q-switch of the Nd:YAG laser. There is an adjustable delay from the trigger pulse to the Q-switch pulse and therefore the signal of the PMT can be stored 200 nsec before the laser is fired. Thus, each captured lidar signal contains a distinct start indication coming from laser beam scattering by the output optics. From these indications it is ensured that the triggering of the transient recorder is exact. In the evaluation of the measurement results the time scale is automatically compensated for the time delay in the recorded data. The triggering of the PMT gain modulation, which in turn is made by the transient recorder, and the shape of the modulation pulse have also been carefully examined and were found to be very reproducible.

Tests were made to determine the signal-to-noise ratio in the NO_2 DIAL measurements. The laser power was comparatively low, 1–2 mJ/pulse, and the studies were made in different industrial and urban environments. In one of the tests the DIAL wavelengths were changed from the absorption and reference wavelengths to two close-lying wavelengths with the same interval, but with an equal NO_2 absorption cross section. We averaged 280 pairs of lidar signals and the DIAL signals were calculated as in an ordinary NO_2 measurement. The program routine for concentration calculations was applied to the result with the differential absorption cross-sectional value normally used, 8.3 cm^{-1} atm^{-1}. The absolute value of the result is an indication of the absolute error in a concentration determination. The recordings also provide information on systematic errors in the DIAL measurements. Figure 2 is a diagram of results from the studies. The absolute statistical error is plotted as a function of the distance for two typical

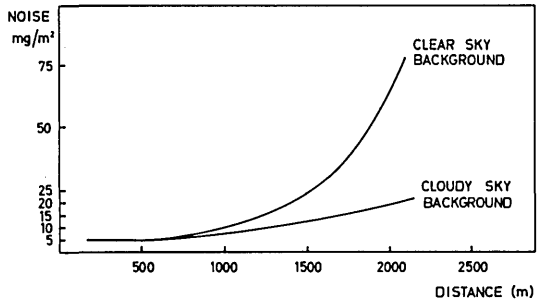

Fig. 2. Absolute statistical error introduced by noise during daytime NO_2 DIAL measurements toward the sky for two typical cases. The error in a measurement of a concentration at a specific distance is given by the value in the diagram divided by the measurement path length. The diagram shows an experimental determination of the error for a low laser power, 1–2 mJ/pulse.

measurement situations, a dry day with a blue sky and a dry day with a cloudy sky. The visibility was estimated to 10 and 4 km, respectively. The systematic error, which is not included in Fig. 2, was found to be very low; much less than the statistical error at the longer distances and definitely <3 mg/m^2 below 1 km. The uncertainty in the exact differential absorption cross section gives, in addition, an accuracy limit of 6%. From the investigations we conclude that the absolute error in a 1-min NO_2 measurement at a distance of 1 km on a dry day with a cloudy sky is 10 mg/m^2, and the accuracy is 6%. The corresponding figures for a measurement with a clear sky background are 13 mg/m^2 and the same accuracy. In some cases when the sky is bright, the lidar can be directed against some distant target to reduce the background light and improve the result. The examples of the statistical error given here are typical for most of the measurement situations studied in this work. In industrial environments with several diffuse plumes and when there is fog, rain, or snow, the signal-to-noise ratio can be worse and there are even uncommon weather conditions when it is not meaningful to do DIAL measurements at all. On the other hand, on clear nights when the background light is extremely low the results can be improved a great deal at the larger distances. Improvements are also made with more laser power, but then at the cost of larger safety ranges, which in some cases can be a restriction.

V. Examples of NO_2 Measurements

During a two and a half-year period the capabilities of the mobile lidar system were extensively investigated in a number of field tests. Measurements were performed in many different measurement situations and a variety of measurement strategies were employed. A few examples of DIAL measurements on NO_2 in industrial and in urban areas will be given here.

Figure 3 shows a daytime NO_2 measurement in a direction through a spreading plume from a nitric acid plant. The lidar system was placed 400 m from the plume. The two diagrams to the left show the backscattered lidar signals at the absorption and reference

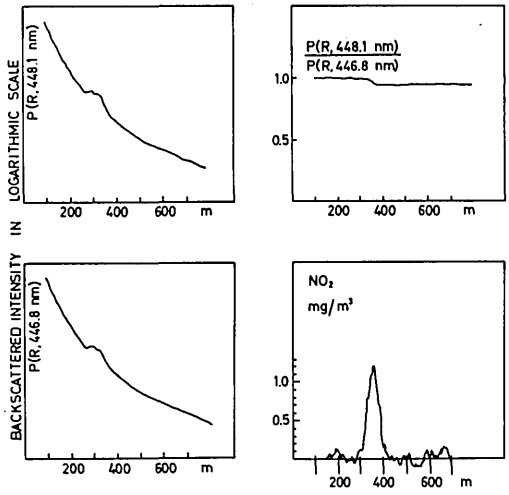

Fig. 3. Example of an NO_2 DIAL measurement through the plume from a stack of a nitric acid plant. The lidar signals at the absorption and reference wavelengths are shown at left, and at upper right the DIAL curve is displayed. The concentration is evaluated with a 50-m path length in the fourth diagram.

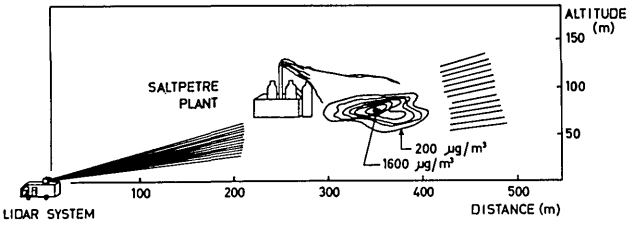

Fig. 4. Charting of the NO_2 content in a plume from a saltpeter plant. The map is drawn from thirteen concentration profiles in different vertical directions.

wavelengths on a logarithmic scale as a function of the distance. We averaged 1100 lidar signals for each of the two curves. The slightly increased signal at 400-m distance is due to particle emissions from another nearby industry. The calculated DIAL signal is displayed at upper right. The evaluation of the concentration, shown in the fourth diagram, was made with a distance resolution of 50 m. From this diagram the noise level is estimated to be 4 mg/m^2 at 500-m distance. The systematic error due to the linear averaging of the lidar recordings, which was discussed in a previous section, is <3%. According to this and the tests performed and discussed in this work the accuracy in the measurement is within 8%.

A charting of the spreading plume is shown in Fig. 4 based on several measurements of the same type as those shown in Fig. 3. The direction for the vertical section is given by the x axis of the diagram. To determine the flow in the plume, which is a very important DIAL application, the NO_2 content in the vertical section of the plume is integrated. Mathematically this means that the concentration is integrated with the distance and for the different vertical directions of the beam. While a charting of the type shown in Fig. 4 takes some time to make, it is possible to do a rapid measurement of the integrated content, since all lidar

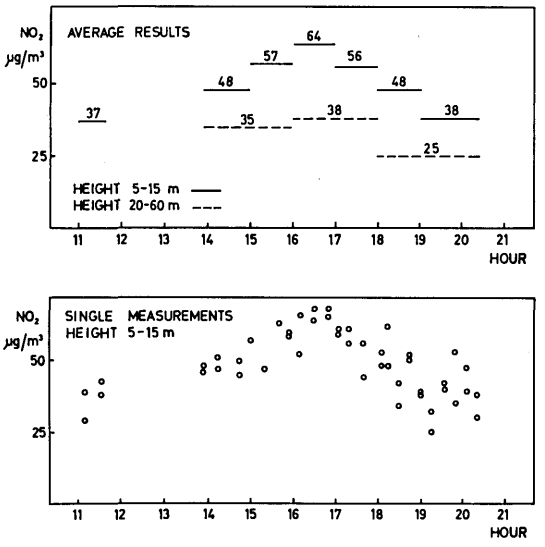

Fig. 5. Diagrams displaying NO_2 DIAL measurements on a street during one day. The lower diagram shows the results of the individual measurements for the 5–15-m height. The upper diagram shows the average results for 1-h periods. Results from DIAL measurements at a greater height are included in the upper diagram. A path length of 500 m was chosen in the study. The measurement project was also a test on the statistical error.

data are then averaged and a good enough signal-to-noise ratio is achieved more quickly. This measurement technique is further discussed in Ref. 5. The integration of the NO_2 concentration in Fig. 4 yields 1.8 (0.2) g/m. The wind speed was 5.6 m/sec, which was measured by an anemometer at the plant, and the angle between the plume and the laser beam was given by the lidar to be 30°. This determined the NO_2 flow to be 5.0 (1.0) g/sec or 18 (4) kg/h, where the accuracy is mainly limited by the uncertainty in the wind-speed value. In this field test the concentration was measured at different distances from the source. We could then observe differences which we attributed to transformation of NO to NO_2. Besides doing regular measurements of flows of NO_2 the subject of atmospheric transformation is an interesting topic where the DIAL technique can be useful.

Motor vehicle traffic is an important source of NO_2. This makes measurements in city streets interesting. The lidar technique has some distinct advantages compared with conventional *in situ* instruments. Such instruments take samples and the sampling procedure may influence the concentration, and further they might accidentally be placed where sudden local maxima make the measurements nonrepresentative. DIAL measurements are performed over several hundred meters, which makes them less sensitive to local fluctuations. It is possible to chart the concentration in a large volume around and/or above the street, which would require a large number of point measuring stations. The diagrams in Fig. 5 show results from measurements during one day on a main street of a medium-size Swedish town. The laser beam was directed along the street and measurements were performed at two different heights (5–15 m and 20–60 m). The average concentrations were evaluated over a 500-m path. In the lower diagram a series of 2-min measurements at the lower height is displayed. To investigate the statistical fluctuations of the concentration the study was performed as four sequential 1-min measurements. The first and third measurements were averaged and likewise the second and fourth measurements. The averaged 2-min measurements are plotted in the diagram. The difference between two such measurements is then due to a combination of changes in the NO_2 concentration in the atmosphere and the statistical noise in the lidar signal. From the diagram it is inferred that the sum of these changes and the statistical noise in this case was $<6\ \mu g/m^3$. The statistical error is then certainly lower than the one discussed in the previous section. In the upper diagram in Fig. 5 the measurements in the study have been averaged for intervals of 1 h in order to give representative values for the concentration. It is obvious that the increased traffic in the late afternoon influences the pollution level.

Figure 6 shows the results of another day of DIAL measurements on a street. The measurement object was a street in Gothenburg, which carries a comparatively heavy traffic load with many diesel trucks. The day was sunny with light winds until 3 p.m. when a

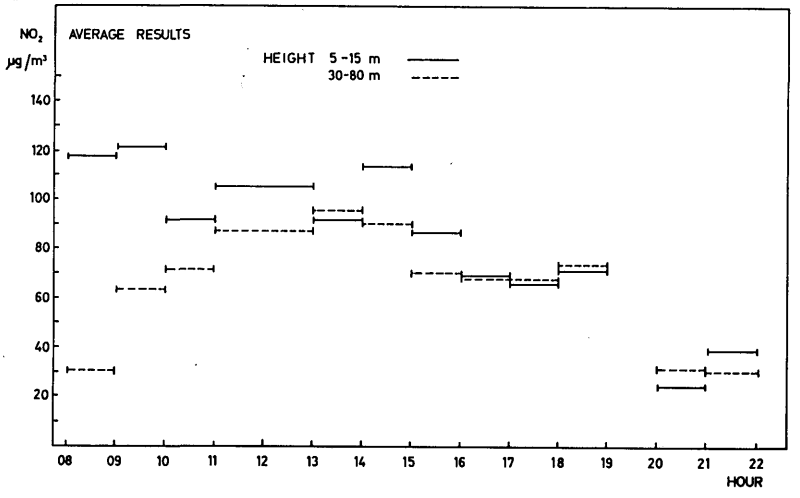

Fig. 6. NO_2 concentrations along a city street with comparatively heavy traffic. The path length was 400 m in the evaluation. The results for two height intervals are shown in the diagram. The atmospheric mixing during the day is manifested.

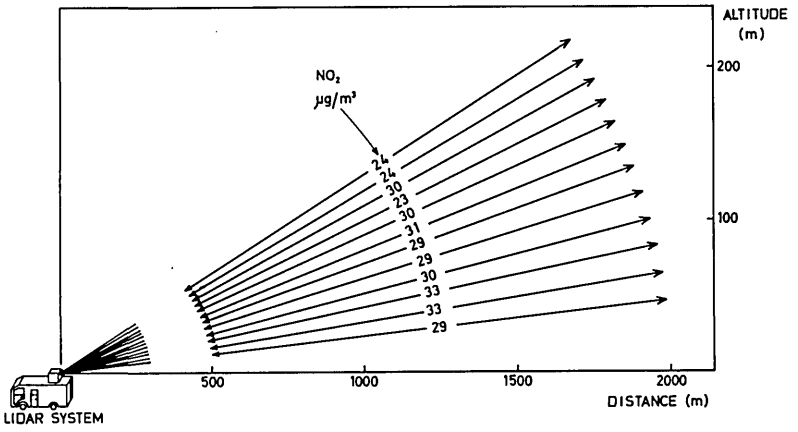

Fig. 7. DIAL measurements on a widespread plume from a metropolitan area. The average concentrations are given in the figure for each direction and the evaluated paths are indicated.

breeze started. During the day, vertical sections were studied, each with 1-min measurements in eight directions. The average concentration was evaluated for the 200–600-m range from the lidar system. Large short-time fluctuations in the concentration were noted, and the highest 1-min average value recorded was 200 $\mu g/m^3$. The figure shows 1-h averages of the concentration in two of the eight measurement directions. The directions displayed are the one closest to street level (height 5–15-m above street level) and one higher (30–80 m). The figure shows that the concentration at the greater height gradually increases to the same concentration as the one close to street level. The breeze, which started at ~3 p.m., prevented the concentration from increasing in the late afternoon.

Figure 7 shows an example from a study on a widespread plume from a metropolitan area. The measurements were made in the south of Sweden some 25 km from Copenhagen, Denmark. When the wind shifted to the direction of this city the NO_2 concentration increased from <10 $\mu g/m^3$ to ~30 $\mu g/m^3$. The example given shows that the concentration is uniform in the vertical section, and in other measurements we noted that this was the case up to an altitude of 250 m where it was drastically reduced. Each value in Fig. 7 is the calculated result from 700 averaged lidar signals, and the statistical fluctuations and errors are obviously low in this study.

VI. Conclusions

This paper describes some of the work performed in the evaluation and testing of a mobile lidar technique. The emphasis is put on the determination of the accuracy in DIAL measurements on NO_2 in field work. It is shown that the capabilities match the measurement needs in many pollution contexts and that the accuracy and detection limits definitely are better than those predicted in some other earlier papers. The systematic errors and signal-to-noise ratios have been carefully examined and typical numbers for these are given. The discussion on the accuracy can to some extent be transferred to DIAL measurements on other gases.

A few applications of NO_2 DIAL measurements are exemplified in this paper but there are certainly more. The monitoring of diffuse and source emissions is an obvious application and, likewise, the measuring of flows from industrial areas. The oxidization of NO into NO_2 in the atmosphere and the spreading of plumes are processes which are important to study, and in these cases the DIAL remote sensing technique can be useful. Long-distance-transported NO_2 is difficult to study with conventional instruments but can be measured at any altitude with this technique. The gas is an important component in traffic-generated pollution, and there are advantages in using a DIAL system to chart the gas in urban areas and especially along city streets. Not least, the remote measuring technique has applications in research into air pollution problems.

The continuing research at our Center is directed toward applications of the DIAL technique for measurements on NO_2, SO_2 and O_3. Recently a large Swedish industry decided to apply the technique for the control of their diffuse and source emissions of SO_2, and our Center will be involved in the construction of the measuring system. Projects to develop the measuring and evaluation routines are also in progress. A somewhat larger mobile laser laboratory is projected for the continuing research program, which includes the extension of the lidar technique for measurements on gases with absorption spectra in the UV and IR wavelength regions. Some of this early work on NO and Hg was reported by the Lund Institute of Technology.[19,20] Recently further studies on NO and CH_4 along city streets were performed. A field test to measure Cl_2 at a chemical plant was made and measurements on HF are prepared in the laboratory work.

The support and encouragement from G. Persson, National Environment Protection Board, and S. Svanberg, Lund Institute of Technology, in the lidar work are gratefully acknowledged. The grants for the work were provided by the Swedish Environment Protection Board and the Swedish Space Corp.

References

1. D. K. Killinger and A. Mooradian, Eds., *Optical and Laser Remote Sensing* (Springer, Berlin, 1983).
2. K. Fredriksson, B. Galle, K. Nyström, and S. Svanberg, Appl. Opt. **18**, 2998 (1979).
3. K. Fredriksson, B. Galle, K. Nyström, and S. Svanberg, Appl. Opt. **20**, 4181 (1981).

4. K. Fredriksson, National Environment Protection Board Report SNV PM 1639 (1982).
5. A.-L. Egebäck, K. Fredriksson, and H. M. Hertz, Appl. Opt. **23,** 722 (1984).
6. K. W. Rothe, U. Brinkman, and H. Walther, Appl. Phys. **3,** 116 (1974); **4,** 181 (1975).
7. W. B. Grant, R. D. Hake, E. M. Liston, R. C. Robbins, and E. K. Proctor, Appl. Phys. Lett. **24,** 550 (1974).
8. R. A. Baumgartner, L. D. Fletcher, and J. G. Hawley, J. Air Pollut. Control Assoc. **29,** 1162 (1979).
9. N. Takeuchi, H. Shimizu, and M. Okuda, Appl. Opt. **17,** 2734 (1978).
10. P.-I. Grennfelt, Institute of Air and Water Research, Göteborg; private communication.
11. E. D. Hinkley, Ed., *Laser Monitoring of the Atmosphere* (Springer, Berlin, 1976).
12. T. Halldorsson and J. Langerholc, Appl. Opt. **17,** 240 (1978).
13. J. Harms, Appl. Opt. **18,** 1559 (1979).
14. K. Sassen and G. C. Dodd, Appl. Opt. **21,** 3162 (1982).
15. W. S. Heaps, in *Proceedings, Eleventh International Laser Radar Conference*, NASA Conf. Publ. 2228, 75 (1982).
16. S. R. Pal and A. I. Carswell, Appl. Opt. **15,** 1990 (1976).
17. A. I. Carswell, Can. J. Phys. **61,** 378 (1983).
18. P. T. Woods and B. W. Jolliffe, Opt. Laser Technol. **10,** 25 (1978).
19. M. Aldén, H. Edner, and S. Svanberg, Opt. Lett. **7,** 543 (1982); H. Edner, K. Fredriksson, H. Hertz, and S. Svanberg, Lund Reports on Atomic Physics, LRAP-21 (1983).
20. M. Aldén, H. Edner, and S. Svanberg, Opt. Lett. **7,** 221 (1982).

Meetings Calendar *continued from page 1398*

1984

June

23–27 Synthetic Aperture Radar Tech. & Applications course, Ann Arbor *U. Mich., Eng. Summer Conf., 200 Chrysler Center, North Campus, Ann Arbor, Mich. 48109*

25–26 Optical Communication Systems NSF Mtg., San Diego *J. Lukas, Electrical Eng. & Computer Sciences Dept., C-014, U. Calif. San Diego, La Jolla, Calif. 92093*

25–27 Flow Visualization Techniques course, Ann Arbor *U. Mich., Eng. Summer Conf., 200 Chrysler Center, North Campus, Ann Arbor, Mich. 48109*

25–27 Forefronts of Large-Scale Computational Problems Conf., Gaithersburg *H. Raveche, A311, Physics Bldg., NBS, Wash., D.C. 20234*

25–28 Ocean Optics VII Conf., Monterey *SPIE, P.O. Box 10, Bellingham, Wash. 98227*

25–29 Measurement of Laser Output Characteristics course, Las Vegas *Eng. Tech., Inc., P.O. Box 8859, Waco, Tex. 76714*

25–29 Advances in Color Tech. course, Rochester *B. Reimherr, One Lomb Memorial Dr., Rochester, N.Y. 14623*

25–29 Computer Vision & Image Processing course, Ann Arbor *U. Mich., Eng. Summer Conf., 200 Chrysler Center, North Campus, Ann Arbor, Mich. 48109*

25–29 NSF Regional Conf.: Factorization of Linear Operators & Geometry of Banach Spaces, U. Missouri, Columbia *NSF, Math. Sciences, Wash., D.C. 20550*

25–29 Advanced Infrared Tech. course, Ann Arbor *U. Mich., Eng. Summer Conf., 200 Chrysler Center, North Campus, Ann Arbor, Mich. 48109*

26–28 Defense Systems Analysis course, Wash., D.C. *Continuing Eng. Ed. Program, Geo. Wash. U., Wash., D.C. 20052*

26–28 Applications of Optical Digital Data Disk Storage Systems Tech. Mtg., Brussels *SPIE, P.O. Box 10, Bellingham, Wash. 98227*

27–3 July Int. Conf. on Plasma Physics, Lausanne *M. Tran, Centre de Recherches en Physique des Plasmas, Ecole Polytechnique Federale, 21, av. des Bains, CH-1007 Lausanne, Switzerland*

July

2–4 2nd Inter. Symp. on Applications of Laser Anemometry to Fluid Mechanics, Lisbon *D. Durao, Dept. of Mechanical Engineering, Instituto Superior Tecnico, Avenida Rovisco Pais, 1096 Lisbon, Portugal*

2–5 Int. Conf. on the Physics of Highly Ionized Atoms, Oxford *P. Hoyng, Astronomical Inst. at Utrecht, Space Research Lab., Beneluxlaan 21-3527 HS, Utrecht, The Netherlands*

2–13 Applied Optics Summer course, London *J. Dainty, Optics Section, Blackett Lab., Imperial College, London SW7, 2BZ, U.K.*

9–12 Radar Signal Processing & Automatic Detection course, Wash., D.C. *Continuing Eng. Ed. Program, Geo. Wash. U., Wash., D.C. 20052*

9–13 Infrared Spectroscopy I: Interpretation of Spectra course, Brunswick *D. Mayo, Chem. Dept., Bowdoin Coll., Brunswick, Maine 04011*

9–13 Mapping From Space: Techniques & Applications course, Wash., D.C. *Continuing Eng. Ed. Program, Geo. Wash. U., Wash., D.C. 20052*

9–13 Laser Fundamentals & Systems course, Wash., D.C. *Eng. Tech., Inc., P.O. Box 8859, Waco, Tex. 76714*

9–20 Lasers & Optics for Applications course, Cambridge *S. Ezekiel, MIT, Elect. Eng. & Computer Science Dept., Cambridge, Mass. 02139*

15–19 Int. Conf. on Laser Processing & Diagnostics—Applications in Electronic Materials, Linz *P. Hoyng, Astronomical Inst. at Utrecht, Space Research Lab., Beneluxlaan 21-3527 HS, Utrecht, The Netherlands*

16–20 NSF Regional Conf.: Geometric Algebra & Ends of Maps, U. Notre Dame, Notre Dame *NSF, Math. Sciences, Wash., D.C. 20550*

16–20 Infrared Spectroscopy II: Instrumentation, Polymer Spectra, Sample Handling & Computer Assisted Spectroscopy course, Brunswick *D. Mayo, Chem. Dept., Bowdoin Coll., Brunswick, Maine 04011*

16–27 Contemporary Optics course, Rochester *E. Snyder, Inst. Optics, U. Rochester, Rochester, N.Y. 14627*

16–27 Optical Metrology course, Viana Do Castelo *O. Soares, Laboratorio de Fisica, Faculdade de Ciencias, Universidade do Porto, 4 000 Porto, Portugal*

22–25 2nd Int. Conf. on Photographic Papers, Vancouver *R. Wood, SPSE, 7003 Kilworth Lane, Springfield, Va. 22151*

23–27 9th Int. Conf. on Atomic Physics, Seattle *G. Wood, Nat. Res. Council Assembly of Mathematical & Physical Sciences, 2101 Constitution Ave., N.W., Wash., D.C. 20418*

continued on page 1424